nature genetics

A synonymous variant in *IRGM* alters a binding site for miR-196 and causes deregulation of IRGM-dependent xenophagy in Crohn's disease

Patrick Brest[1,2], Pierre Lapaquette[3,4], Mouloud Souidi[5,6], Kevin Lebrigand[2,7], Annabelle Cesaro[1,2], Valérie Vouret-Craviari[1,2], Bernard Mari[2,7], Pascal Barbry[2,7], Jean-François Mosnier[8], Xavier Hébuterne[1,2,9], Annick Harel-Bellan[5,6], Baharia Mograbi[1,2], Arlette Darfeuille-Michaud[3,4,12] & Paul Hofman[1,2,10–12]

Susceptibility to Crohn's disease, a complex inflammatory disease, is influenced by common variants at many loci. The common exonic synonymous SNP (c.313C>T) in *IRGM*, found in strong linkage disequilibrium with a deletion polymorphism, has been classified as non-causative because of the absence of an alteration in the IRGM protein sequence or splice sites. Here we show that a family of microRNAs (miRNAs), miR-196, is overexpressed in the inflammatory intestinal epithelia of individuals with Crohn's disease and downregulates the *IRGM* protective variant (c.313C) but not the risk-associated allele (c.313T). Subsequent loss of tight regulation of IRGM expression compromises control of intracellular replication of Crohn's disease–associated adherent invasive *Escherichia coli* by autophagy. These results suggest that the association of *IRGM* with Crohn's disease arises from a miRNA-based alteration in IRGM regulation that affects the efficacy of autophagy, thereby implicating a synonymous polymorphism as a likely causal variant.

The *IRGM* region contains multiple polymorphisms that cause tissue-specific variation in *IRGM* expression[1–3]. A synonymous variant within the *IRGM* coding region (rs10065172, NM_001145805.1, c.313C>T) in perfect linkage disequilibrium ($r^2 = 1.0$) with a 20-kb deletion upstream of *IRGM* has been strongly associated with Crohn's disease in individuals of European descent[1,4,5]. A recent study proposed that allelic differences in the promoter region might be involved in Crohn's disease pathogenesis[1], as the deletion, and other copy number variants, closely juxtapose several transcription factor binding sites[2]. An alternative hypothesis is that the synonymous exonic (CTG>TTG, leucine) variant might affect protein expression. In this regard, recent evidence that a polymorphism can alter miRNA-directed repression of mRNA in a 3′ untranslated region[6,7] is of particular interest. Thus, we investigated whether miRNA binding to *IRGM* mRNA could be defective in subjects with the T allele and consequently lead to abnormal regulation of IRGM expression.

For this purpose, we assessed binding of miRNAs to the different forms of *IRGM* mRNA *in silico* using SnipMir, RegRNA and Patrocles software (see URLs). We observed a predicted loss in binding of two miRNAs, miR-196A and miR-196B, to the risk haplotype carrying the T allele (**Fig. 1a**). Indeed, the c.313C>T polymorphism of *IRGM* is located within the 'seed' region, where mRNA-miRNA forms a complex within RISC (RNA-induced silencing complex), which is important for mRNA regulation. Two pre–miR-196A genes (*MIR196A1* and *MIR196A2*) encode the same mature miR-196A, whereas miR-196B (*MIR196B*) is unique within the genome (**Supplementary Note**). Both miRNAs share the same 'seed' region and target specificity. Moreover, tandem affinity purification of miRNA target mRNA (TAP-Tar)[8] showed higher binding of miR-196 to *IRGM* c.313C mRNA (hereafter $IRGM^C$) than to *IRGM* c.313T mRNA (hereafter $IRGM^T$), confirming *in silico* predictions (**Fig. 1b**). In HEK293 cells (C/C for rs10065172), miR-196 transfection decreased protein expression from a FLAG-tagged $IRGM^C$ construct as well as endogenous IRGM protein levels, whereas expression from a FLAG-tagged $IRGM^T$ construct remained constant (**Fig. 1c**). Using a modified miR-196 (miR-196^{MOD}) with a compensatory c.3G>A mutation (**Supplementary Note**), we observed stronger binding to $IRGM^T$ than to $IRGM^C$ and a concomitant decrease in protein expression from the FLAG-tagged $IRGM^T$ construct (**Supplementary Fig. 1**). Together, these results indicate that the Crohn's disease–associated risk (T allele) and protective (C allele) haplotypes confer differences in IRGM expression under the control of miR-196. Notably, the miR-196 family and the miR-196 binding site within the coding sequence of *IRGM* family members are conserved in

[1]INSERM ERI-21, EA4319, Faculty of Medicine, Nice, France. [2]University of Nice Sophia Antipolis, Nice, France. [3]Clermont Université, Université d'Auvergne, Jeune Equipe JE 2526, Clermont-Ferrand, France. [4]INRA, Institut de Recherche Agronomique, Unité sous contrat USC-2018, Clermont-Ferrand, France. [5]Université Paris-Sud 11, Epigenetics and Cancer, FRE 3239, Villejuif, France. [6]Centre National de la Recherche Scientifique (CNRS), Villejuif, France. [7]CNRS UMR 6097, Institut de Pharmacologie Moléculaire et Cellulaire, Valbonne, France. [8]EA4273, University of Nantes, Nantes, France. [9]Centre Hospitalier Universitaire de Nice, Hôpital de l'Archet, Service de Gastroentérologie, Nice, France. [10]Centre Hospitalier Universitaire de Nice, Hôpital Pasteur, Tumorothèque, Centre de Ressource Biologique INSERM, Nice, France. [11]Centre Hospitalier Universitaire de Nice, Hôpital Pasteur, Laboratoire de Pathologie Clinique et Expérimentale, Nice, France. [12]These authors contributed equally to this work. Correspondence should be addressed to P.H. (hofman@unice.fr) or A.D.-M. (arlette.darfeuille-michaud@u-clermont1.fr).

Received 1 October 2010; accepted 10 January 2011; published online 30 January 2011; doi:10.1038/ng.762

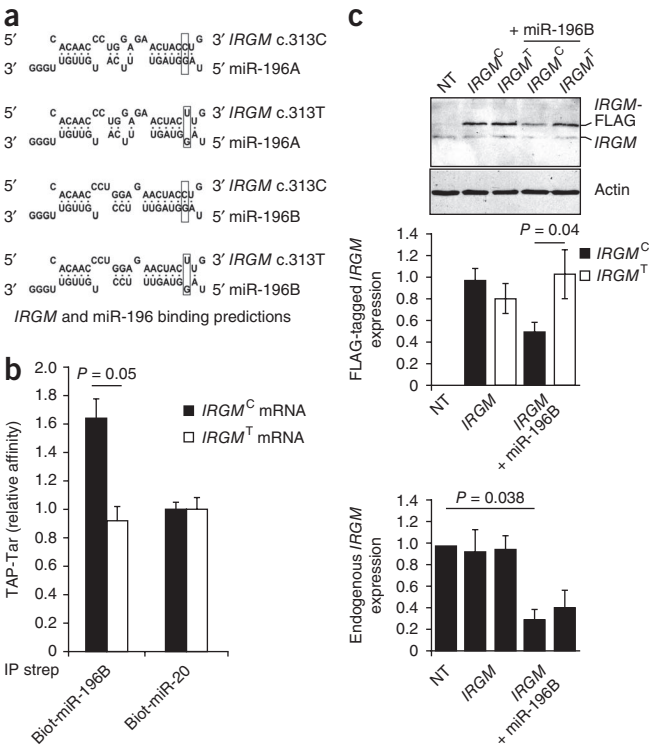

Figure 1 Allele-specific regulation of *IRGM* by miR-196. (**a**) *In silico* prediction of miR-196 and *IRGM* mRNA interactions showed differences in binding within the seed region. (**b**) $IRGM^C$ mRNA was significantly enriched in miR-196B complexes. Extracts of cells expressing FLAG-tagged-AGO1 and transfected with biotinylated miR-196B or control miR-20 as indicated and then with $IRGM^C$ or $IRGM^T$ plasmids were submitted to tandem affinity purification (immunoprecipitation with FLAG antibodies followed by affinity purification on streptavidin beads). *IRGM* mRNA variants were quantified using quantitative RT-PCR; results are presented as the ratio between miR-196B and miR-20 (non-relevant miRNA) pull-downs and the mean of three independent experiments ± standard deviation (s.d.). IP strep, immunoprecipitation straptavidine. (**c**) HEK293 cells ($IRGM^{C/C}$) were transfected with either FLAG-tagged $IRGM^C$ or FLAG-tagged $IRGM^T$ plasmids and co-transfected with miR-196B. Immunoblotting with an IRGM antibody revealed the specificity of the downregulation effect mediated by the miRNA *IRGM* mRNA interaction. Quantification of the immunoblot signals are presented as IRGM expression relative to actin (mean of at least three independent experiments ± s.d.).

different species, suggesting that control of IRGM protein expression by miR-196 is under evolutionary constraint (**Supplementary Fig. 2**).

To correlate *in silico* and *in vitro* data with the pathophysiology of Crohn's disease, we analyzed expression of miR-196 in human biopsies using *in situ* hybridization and fractional laser capture microdissection followed by quantitative PCR. Increased expression of miR-196 was restricted to intestinal epithelial cells within inflamed ileum and colon in individuals with Crohn's disease compared to healthy controls, as shown by representative images of global staining for miR-196 by *in situ* hybridization (**Fig. 2a** and **Supplementary Fig. 3**). To confirm these data, we determined expression levels of miR-196A and miR-196B in epithelial and lamina propria fractions isolated by laser capture microdissection (**Supplementary Fig. 4**). Notably, expression of miR-196A and miR-196B in the epithelium (relative to that in the lamina propria) was lower in healthy tissue from control individuals or individuals with Crohn's disease and was progressively increased in quiescent and inflamed tissues from individuals with Crohn's disease (**Fig. 2b** and **Supplementary Fig. 5**) independently of *IRGM* c.313C or

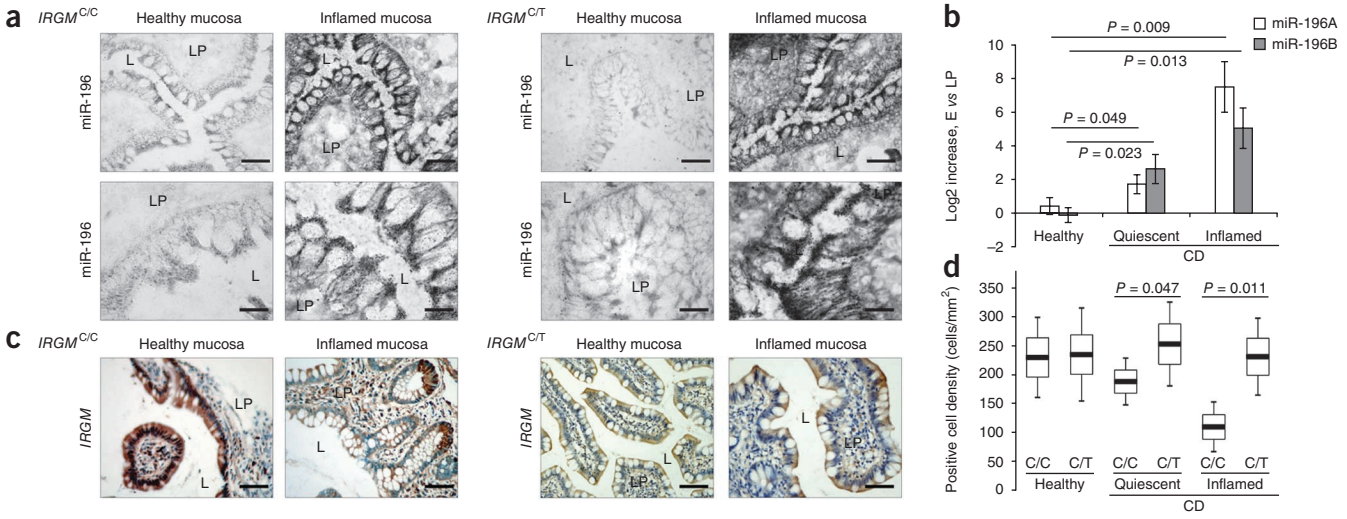

Figure 2 miR-196 overexpression in inflamed mucosa correlates with decreased expression of the *IRGM* c.313C variant *ex vivo*. (**a**) Representative *in situ* hybridization of frozen sections obtained from colon biopsies of genotyped healthy controls ($n = 40$) or individuals with Crohn's disease (CD) ($n = 67$) without or with active inflammation and labeled for miR-196A. (L, lumen; LP, lamina propria). Scale bars in the upper panel, 25 µm; scale bars in the lower panel, 10 µm. (**b**) Epithelial or laminal fractions were captured from sections of biopsies of healthy controls ($n = 8$) or individuals with Crohn's disease with no inflammation ($n = 16$), quiescent (defined as low-grade inflammation) ($n = 8$) or acute inflammation ($n = 8$) using laser capture microdissection. After RNA extraction, miR-196A (black bars) and miR-196B (white bars) relative expression was analyzed using RNU19, 44 and U6. To overcome possible inter-individual bias, the lamina propria fraction value was used for relative quantification. Due to high differences in expression between healthy and inflamed tissues, the results are presented as a log2-fold ratio. Error bars indicate the s.d. of the ΔΔCt values. (**c**) Representative *in situ* staining for IRGM of TMAs from colon biopsies of healthy individuals or individuals with Crohn's disease with a defined genotype in a healthy non-inflamed or an acute inflamed phase. Scale bars, 32 µm. (**d**) Mean (black line), s.e.m. (white box) and 95% CI of the mean of the IRGM expression level for 40 healthy subjects (32 individuals with C/C and 8 individuals with C/T) and 67 individuals with Crohn's disease (45 with C/C and 22 with C/T) with quiescent or inflamed colon mucosa. We performed statistical analysis using ANOVA ($P = 0.0015$) and an unpaired Student's *t*-test (the one tail *P* value is indicated on the figure).

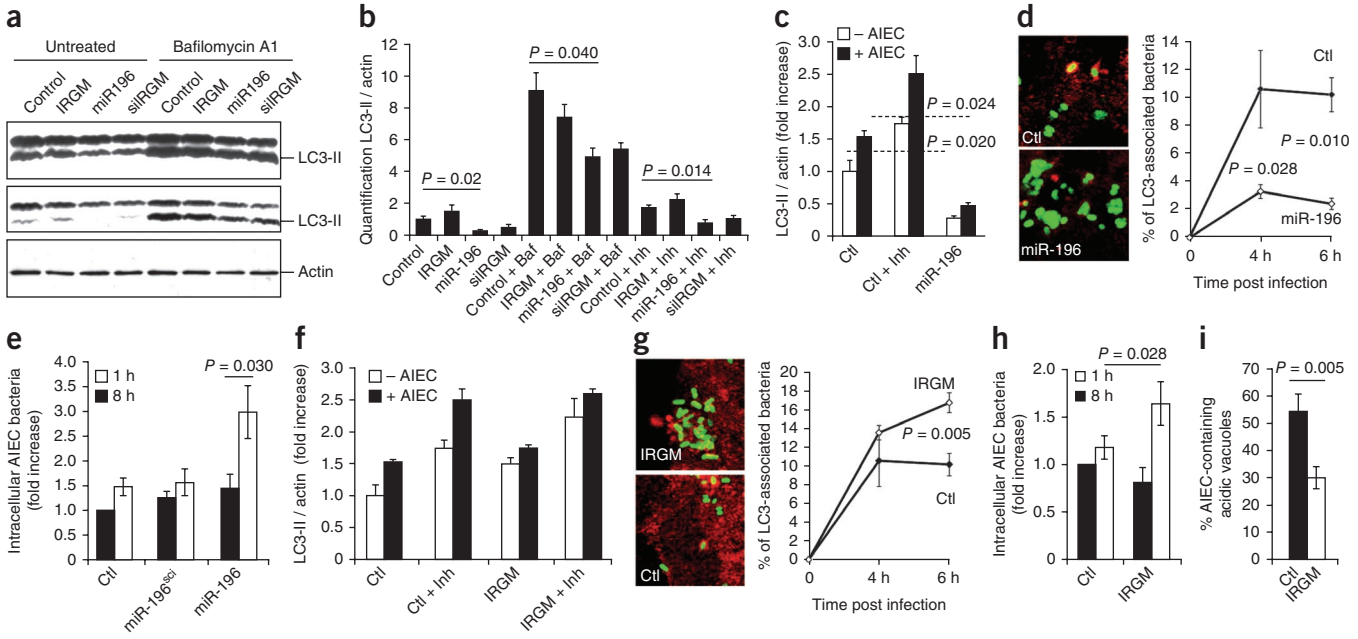

Figure 3 IRGM expression and miR-196 affect autophagic flux and AIEC-bacteria–mediated autophagy. (**a**) The basal flux of autophagy is affected by IRGM expression level. HEK293 cells transfected with an IRGM-expressing plasmid, miR-196 or siIRGM were treated with bafilomycin A1 for 2 h and processed for immunoblotting with anti-LC3B. (**b**) Quantification of LC3-II relative to actin (mean of three independent experiments ± s.d.). (**c**) Downregulation of IRGM expression by miR-196 abrogates AIEC-mediated autophagy in cells treated with autophagic inhibitors (Inh) or transfected with miR-196B and infected for 4 h with AIEC LF82 (mean of three independent experiments ± s.d.). (**d**) Confocal microscopic examination of LC3 revealed a significant decrease in the percentage of LC3-associated (red) LF82 bacteria (green) in miR-196 transfected cells compared to control cells (mean ± s.d.). (**e**) miR-196 transfection leads to increased intracellular LF82 replication. Results are expressed as a fold increase ± s.e.m. of intracellular bacteria. (**f**) IRGM overexpression did not inhibit autophagic flux and it increased LC3-II accumulation slightly in response to AIEC infection. HEK293 cells were transfected with IRGM-expressing plasmid, treated with autophagic inhibitors and infected with AIEC bacteria for 4 h (mean of three independent experiments ± s.d.). (**g**) Confocal microscopic examination showed an increased percentage of LC3-associated AIEC bacteria in IRGM cells compared to control cells (mean ± s.d.). (**h**) IRGM overexpression led to a high rate of intracellular replication of LF82 bacteria. (**i**) Most of the bacteria reside in non-acidic vacuoles, as shown with lysotracker at 8 h post infection (means of three independent experiments ± s.d.).

T allelic status (**Supplementary Note** and **Supplementary Table 1**). We investigated whether the increase in miRNA expression could be a consequence of stimulation by bacterial components or cytokines, as previously reported for various cell lines[9–12]. However, *in vitro* experiments indicated no variation in either miR-196A or miR-196B under pro-inflammatory cytokine stimulation (IFN-γ) or infection of HEK293 cells with Crohn's disease–associated adherent invasive *E. coli* (AIEC) bacteria (**Supplementary Fig. 6**).

Next, we analyzed the correlation between miR-196 and IRGM protein expression in epithelial cells within the human intestinal mucosa in tissue microarrays (TMAs) from individuals with Crohn's disease. Representative immunostaining images from colons of individuals with Crohn's disease are shown in **Figure 2c**. In healthy mucosa, IRGM basal expression was strongly positive in epithelial cells independent of genotype and only weakly positive in the lamina propria. Notably, in active mucosa, a decrease in IRGM expression was restricted to epithelial cells of individuals with the *IRGM*$^{C/C}$ genotype. However, when the T allele was present in individuals with Crohn's disease, IRGM expression was maintained under inflammatory conditions (**Fig. 2c**,**d**, **Supplementary Note** and **Supplementary Figs. 3**,**7** and **8**). Thus, our findings show that miR-196 expression in inflammatory conditions correlates with downregulated IRGM expression in human epithelial cells. Of note, IRGM staining was maintained at a high level in Paneth cells (**Fig. 2c** and **Supplementary Fig. 9**), indicating a possible difference in IRGM regulation in these cells. Together with a previous report showing that the levels of autophagy-related proteins ATG16L1 and ATG5 were critical in maintaining normal granule biogenesis[13], we hypothesize that alternative mechanisms regulating autophagy-related events could exist in Paneth cells.

IRGM encodes an autophagic protein that plays an important role in innate immunity against intracellular pathogens like *Mycobacterium tuberculosis*, *Salmonella typhimurium* and Crohn's disease–associated AIEC bacteria[1,14,15]. Compelling evidence indicates that a critical threshold of IRGM can regulate the efficiency of the autophagic process[1,14], but the mechanism of regulation of human IRGM expression remains unknown[3,16]. Thus, we investigated whether miR-196 and subsequently modified IRGM expression might influence basal autophagic flux by monitoring LC3-II conversion. LC3-II levels decrease during prolonged autophagy due to its degradation after autophagosomal-lysosomal fusion, so we measured the flux through the autophagic system by comparing LC3-II levels in the presence or absence of lysosomal inhibitors that partially (pepstatin + E64D) or completely (bafilomycin A1) prevent LC3-II degradation. Notably, miR-196, which reduced IRGM expression (**Fig. 1**), induced a significant decrease in LC3-II conversion (**Fig. 3a**,**b**; $P = 0.02$). Moreover, when autophagy was blocked with lysosomal inhibitors, miR-196 inhibited the accumulation of LC3-II (**Fig. 3a**,**b**), which suggests strongly that miR-196 overexpression inhibits the autophagic process at the initiation step.

To determine the effect of the increase in miR-196 expression observed in individuals with Crohn's disease, we examined the autophagic flux in response to Crohn's disease–associated AIEC infection. In response to AIEC bacterial infection, we observed increased formation of LC3-II (**Fig. 3c**). When we blocked lysosomal LC3-II degradation, we observed a larger increase in LC3-II in AIEC-infected

cells, indicating functional autophagic flux. In miR-196 transfected cells, we noted a decrease in autophagic flux (**Fig. 3b**,**c**) associated with decreased numbers of LC3-II–associated bacteria (**Fig. 3d**; $P = 0.01$) and a significantly ($P = 0.03$) higher number of intracellular AIEC LF82 bacteria (**Fig. 3e** and **Supplementary Fig. 10**). Of note, we observed similar results in cells infected with IRGM small interfering RNA (siRNA) (**Supplementary Fig. 11**) but not in cells transfected with miR-196^{MOD} or miR-196^{sc} (**Supplementary Note** and **Supplementary Fig. 12**). Thus, miR-196 may act in endogenous fine-tuning of the initiation of the autophagic pathway and in the control of intracellular pathogen degradation in human cells by regulating IRGM expression.

According to the data shown above (**Fig. 2**), the absence of regulation of *IRGM*^{T} by miR-196 is concomitant with sustained IRGM protein expression in intestinal epithelial cells. Analysis of IRGM localization and autophagic flux in HEK293 cells overexpressing the IRGM protein indicated unchanged compartmentalization (**Supplementary Fig. 13**) and a normal basal autophagic flux as shown by the LC3-II to actin ratio (**Fig. 3a**,**b**). As IRGM overexpression leads to an increase in intracellular *Salmonella* spp. targeted by the autophagic machinery[1], we conducted experiments with AIEC bacteria. HEK293 cells overexpressing the IRGM protein exhibited induction of autophagy in response to AIEC infection, as shown by the LC3-II to actin ratio (**Fig. 3f**). In addition, IRGM overexpression was associated with increased numbers of LC3-II–associated bacteria ($P = 0.005$), which was more pronounced at 6 h post infection (**Fig. 3g**), together with an increased number of intracellular AIEC bacteria (**Fig. 3h** and **Supplementary Fig. 14**). Irgm1, the mouse ortholog of IRGM, has been reported to be associated with the membrane of the phagosome and to be involved in phagosome full maturation[17]. We therefore analyzed whether AIEC bacteria co-localized with acidic vacuoles in cells overexpressing IRGM. Using the lysotracker probe, we observed a significant decrease in the percentage of AIEC LF82 bacteria in acidic compartments in cells overexpressing IRGM compared to non-transfected cells (**Fig. 3i** and **Supplementary Fig. 15**). Taken together, our data show that miR-196 controls the level of IRGM, which is critical for both the initiation and the maturation of xenophagy.

Our results provide an explanation for the potential consequence of the *IRGM* c.313C>T polymorphism, which, along with other polymorphisms, creates tissue-specific variation in IRGM expression and influences predisposition to inflammatory bowel disease in individuals of European ancestry. Indeed, by showing that this synonymous variant alters a miRNA binding site, we provide evidence for inflammatory-dependent loss of regulation of the autophagy-related protein IRGM in individuals with the Crohn's disease risk haplotype. We speculate that AIEC infection in individuals with miR-196–dysregulated IRGM expression (c.313T carriers) leads to altered antibacterial activity of intestinal epithelial cells and abnormal persistence of Crohn's disease–associated intracellular bacteria, with a substantial impact on the outcome of intestinal inflammation. Finally, our data provide the first example, to our knowledge, of a miRNA-associated synonymous polymorphism influencing human disease risk.

URLs. SnipMir, http://www.microarray.fr:8080/merge/index?action=MISNP ; RegRNA, http://regrna.mbc.nctu.edu.tw/ ; Patrocles, http://www.patrocles.org/.

METHODS

Methods and any associated references are available in the online version of the paper at http://www.nature.com/naturegenetics/.

Accession codes. The human *IRGM* data from this study is deposited in GenBank with the accession code A1A4Y4.

Note: Supplementary information is available on the Nature Genetics website.

ACKNOWLEDGMENTS

This work was supported by grants from the Ministère de la Recherche et de la Technologie (JE2526, A.D.-M.), by INRA (USC 2018, A.D.-M.) by the Association F. Aupetit (A.D.-M. and V.V.-C.), by the Institut National du Cancer (07/3D1616/Pdoc-110-32/NG-NC (P. Brest), PL0079 (P. Barbry) and INFLACOL (P.H.)), the European Community (P. Barbry and B. Mari; MICROENVIMET, FP7-HEALTH-F2-2008-201279), Association pour la Recherche sur le Cancer (ARC), Villejuif, France (V.V.-C.), Integrated Project SIROCCO LSHG-CT-2006-037900 (A.H.-B.), French clinical research projects funding program 'MUTCROHN' (PHRC-2010) (X.H.) and the Infectiopôle Sud PACA (P.H.). The confocal microscope was the property of the Université d'Auvergne. The authors would like to thank E. Selva, V. Gavric-Tanga, K. Havet, O. Bordone, G. Cane, M. Ohanna and A. Chargui for their excellent technical assistance.

AUTHOR CONTRIBUTIONS

P. Brest, B. Mograbi, A.D.-M. and P.H. designed the study. P. Brest, P.L., M.S. and A.C. performed the experiments. P. Brest, P.L., M.S., B. Mograbi, A.D.-M. and P.H. collected and analyzed the data. P.H., J.-F.M. and X.H. participated in subject recruitment and in the Tissue Bank. P. Brest, P.L., A.H.-B., B. Mograbi, A.D.-M. and P.H. wrote the manuscript. K.L., V.V.-C., A.H.-B., B. Mari and P. Barbry gave technical support and conceptual advice.

COMPETING FINANCIAL INTERESTS

The authors declare no competing financial interests.

Published online at http://www.nature.com/naturegenetics/.
Reprints and permissions information is available online at http://npg.nature.com/reprintsandpermissions/

1. McCarroll, S.A. *et al.* Deletion polymorphism upstream of *IRGM* associated with altered *IRGM* expression and Crohn's disease. *Nat. Genet.* **40**, 1107–1112 (2008).
2. Prescott, N.J. *et al.* Independent and population-specific association of risk variants at the *IRGM* locus with Crohn's disease. *Hum. Mol. Genet.* **19**, 1828–1839 (2010).
3. Bekpen, C. *et al.* Death and resurrection of the human *IRGM* gene. *PLoS Genet.* **5**, e1000403 (2009).
4. Parkes, M. *et al.* Sequence variants in the autophagy gene *IRGM* and multiple other replicating loci contribute to Crohn's disease susceptibility. *Nat. Genet.* **39**, 830–832 (2007).
5. Brest, P. *et al.* Autophagy and Crohn's disease: at the crossroads of infection, inflammation, immunity, and cancer. *Curr. Mol. Med.* **10**, 486–502 (2010).
6. Abelson, J.F. *et al.* Sequence variants in *SLITRK1* are associated with Tourette's syndrome. *Science* **310**, 317–320 (2005).
7. Yu, Z. *et al.* Aberrant allele frequencies of the SNPs located in microRNA target sites are potentially associated with human cancers. *Nucleic Acids Res.* **35**, 4535–4541 (2007).
8. Nonne, N., Ameyar-Zazoua, M., Souidi, M. & Harel-Bellan, A. Tandem affinity purification of miRNA target mRNAs (TAP-Tar). *Nucleic Acids Res.* **38**, e20 (2010).
9. O'Connell, R.M., Taganov, K.D., Boldin, M.P., Cheng, G. & Baltimore, D. MicroRNA-155 is induced during the macrophage inflammatory response. *Proc. Natl. Acad. Sci. USA* **104**, 1604–1609 (2007).
10. Zhou, R. *et al.* NF-κB p65-dependent transactivation of miRNA genes following *Cryptosporidium parvum* infection stimulates epithelial cell immune responses. *PLoS Pathog.* **5**, e1000681 (2009).
11. Moschos, S.A. *et al.* Expression profiling *in vivo* demonstrates rapid changes in lung microRNA levels following lipopolysaccharide-induced inflammation but not in the anti-inflammatory action of glucocorticoids. *BMC Genomics* **8**, 240 (2007).
12. Pedersen, I.M. *et al.* Interferon modulation of cellular microRNAs as an antiviral mechanism. *Nature* **449**, 919–922 (2007).
13. Cadwell, K. *et al.* A key role for autophagy and the autophagy gene *Atg16l1* in mouse and human intestinal Paneth cells. *Nature* **456**, 259–263 (2008).
14. Singh, S.B., Davis, A.S., Taylor, G.A. & Deretic, V. Human IRGM induces autophagy to eliminate intracellular mycobacteria. *Science* **313**, 1438–1441 (2006).
15. Lapaquette, P., Glasser, A.L., Huett, A., Xavier, R.J. & Darfeuille-Michaud, A. Crohn's disease-associated adherent-invasive *E. coli* are selectively favoured by impaired autophagy to replicate intracellularly. *Cell. Microbiol.* **12**, 99–113 (2010).
16. Bekpen, C. *et al.* The interferon-inducible p47 (IRG) GTPases in vertebrates: loss of the cell autonomous resistance mechanism in the human lineage. *Genome Biol.* **6**, R92 (2005).
17. MacMicking, J.D., Taylor, G.A. & McKinney, J.D. Immune control of tuberculosis by IFN-gamma-inducible LRG-47. *Science* **302**, 654–659 (2003).

ONLINE METHODS

Cell lines, miRNA and plasmid transfection. HeLa and HEK293 cells were obtained from the European Collection of Cell Cultures (ECACC, Sigma-Aldrich) and grown according to the supplier's recommendations. Pre-miRNA, miRNA precursors of miR-CON1 (Control) and all other miR-196 were purchased from Ambion (Applied Biosystems). siRNA duplexes directed against human *IRGM* were purchased from Invitrogen (HSS156156, Stealth siRNA). Control duplexes were purchased from the same supplier and were GC-matched, non-targeting sequences. HEK293 cells were transfected with miRNA or siRNA using Lipofectamine RNAiMAX (Invitrogen) for 48 h according to the manufacturer's protocol for this cell line. The empty plasmid pCMV and plasmid pCMV-3xFlag-IRGM have been described previously[1,18]. Site-directed mutagenesis of p.Cys313Thr was performed using the QuickChange II site-directed mutagenesis kit (Stratagene, Agilent Technologies). Mutagenesis and clone selection was assessed by allelic discrimination of *IRGM*, and resequencing was done with specific primers as described above. HEK293 cells were transfected with plasmids using Lipofectamine LTX (Invitrogen) for 20 h according to the manufacturer's protocol for this cell line. Immunoblotting was done using antibodies to actin (Sigma), IRGM NT or IN (ProSci) and the appropriate HRP-conjugated secondary antibody (Santa Cruz Biotechnology).

Tandem affinity purification of miRNA target mRNAs (TAP-Tar). HeLa S3 (XLP) cells were cultured with Dulbecco's Modified Eagle's Medium (Invitrogen) containing 10% FCS. The HeLa S3 cell lines stably expressing Flag-HA-AGO1 or Flag-HA-AGO2 were obtained using retroviral vectors as previously described[8]. Cells were transfected with synthetic miRNA (15 nM) miR-196B-WT, miR-196B-MOD and miR-20A biotinylated at the 3′ end with a C10O4 spacer (purchased from Sigma-Aldrich), and the pCMV plasmid containing $IRGM^{C}$ or $IRGM^{T}$ (250 ng) was transfected into cells using HiPerFect (Qiagen) according to the manufacturer's instructions. After tandem purification, total RNA was reverse transcribed and IRGM expression was monitored using allelic discrimination PCR.

Study subjects, biopsy specimens and histology. All subjects included in this study were hospitalized in the Department of Gastroenterology (Archet Hospital, Nice, France). Clinical information regarding associated gastrointestinal and non-gastrointestinal symptoms was obtained from the hospital information system. All individuals included in this study provided a signed agreement, and the protocol was approved by the local ethics committee of the University of Nice Sophia Antipolis, Nice, France (N°UNS-CHUN 2009-25). There were 160 French individuals included in the study (120 with Crohn's disease and 40 controls). The endoscopic index of severity was evaluated for each individual according to the Mary and Modigliani method[19]. For measurement of histological disease activity, the scoring system for histological abnormalities in Crohn's disease mucosal biopsy specimens was used[20]. For each individual included in this series, seven supplementary intestinal biopsies from each area were taken. Three biopsies were used to set up tissue microarrays (TMAs). The latter biopsies were fixed in 10% buffered formalin and then processed, oriented on their edge, embedded in paraffin, cut into sequential 4 µm sections and stained with hematoxylin and eosin. Other biopsies were immediately snap frozen in liquid nitrogen for mRNA extraction (three biopsies). The *IRGM* genotype was first examined using a TaqMan discrimination assay (rs10065172) and a 7500 Fast PCR instrument (Applied Biosystems). The genomic DNA of individuals was re-analyzed by amplification and sequencing (**Supplementary Note**). FLAG-tagged *IRGM* plasmids were used as controls.

miRNA *in situ* hybridization. To investigate the cell-specific distribution of miRNA in normal and inflamed tissues, *in situ* hybridization was performed using 5′ and 3′ end digoxigenin (DIG)–labeled locked nucleic acid (LNA)-modified DNA oligonucleotides (LNAs) complementary to the mature miRNA (Exiqon A/S) following the manufacturer's instructions (**Supplementary Note**). In this study, the global expression of miR-196A was examined in intestinal biopsies (LNA-miR-196A and LNA-scrambled as a negative control).

Tissue microarray (TMA) construction and immunohistochemistry. Representative intestinal biopsies of each individual were selected from hematoxylin and eosin–stained sections for building TMAs. TMAs were set up as previously described[21,22] (**Supplementary Note**). Immunohistochemical methods were performed using anti-IRGM-IN or NT (ProSci Incorporated) or anti-lysozyme (DAKO Envision System, DAKO Corp.) antibodies as previously described[21–23]. IRGM antibody specificity was confirmed by immunoblotting (**Supplementary Fig. 16**).

Laser capture microdissection. Snap-frozen tissue blocks of intestinal biopsies were chosen from the tissue bank of the Human Tissue Biobank Unit, Nice, France and included in Cryomatrix (Thermo Fisher Scientific). Four- to eight-micron serial frozen sections were microdissected using a PixCell laser capture microscope (Arcturus Engineering). After visual control of the completeness of dissection (**Supplementary Fig. 5**), miRNA from the captured tissue was obtained with the MicroRNA isolation kit (Stratagene).

Autophagic flux assay. Autophagic flux was blocked by incubating cells with pharmacological inhibitors bafilomycin A1 (100 nM, Sigma-Aldrich) or pepstatin + E64d (10 mM, Sigma-Aldrich) 30 min before cell infection and kept for the entire duration (4 h) of the experiment. Cells were processed for immunoblotting by loading 25 µg of the proteins, separated on a 15% SDS-PAGE, and then transferred onto a polyvinylidene fluoride membrane. LC3-II accumulation was revealed using LC3-B antibody (Sigma-Aldrich). Anti-actin (Sigma-Aldrich), as loading control, and anti-IRGM (ProSci), as an experimental control, were also used. Quantification was performed using ImageJ software.

Invasion and intracellular survival assay. Bacterial invasion of human epithelial HEK293 cells was performed using the gentamycin protection assay[24]. Monolayers were infected for 3 h at a multiplicity of infection (MOI) of 10 bacteria per cell. At 1 h and 8 h post infection, the number of intracellular bacteria was determined by counting the number of colony-forming units (CFU). Experiments were independently carried out at least three times, and one representative dataset of three independent experiments was presented where appropriate.

Fluorescence microscopy. At indicated times after bacterial infection, HEK293 cells were fixed with 4% paraformaldehyde and immunostained with anti-IRGM-NT (ProSci), anti-LC3 (MBL) and with appropriate secondary antibodies (Invitrogen). Staining of acidic compartments was carried out by incubating cells for 1 h before fixation in medium containing 100 nM of acidotropic dye LysoTracker Red DND99 (Invitrogen). The slides were examined with a Zeiss LSM 510 Meta confocal microscope. Counting was done at ×63 magnification, and at least 100 cells were counted for each experimental condition.

Statistical analysis. Results were evaluated for statistical significance with the Student's *t*-test. Error bars represent the standard deviation of the mean. *P* values less than 0.05 were regarded as significant.

18. Kuballa, P., Huett, A., Rioux, J.D., Daly, M.J. & Xavier, R.J. Impaired autophagy of an intracellular pathogen induced by a Crohn's disease associated ATG16L1 variant. *PLoS ONE* **3**, e3391 (2008).
19. Mary, J.Y. & Modigliani, R. Development and validation of an endoscopic index of the severity for Crohn's disease: a prospective multicentre study. Groupe d'Etudes Therapeutiques des Affections Inflammatoires du Tube Digestif (GETAID). *Gut* **30**, 983–989 (1989).
20. D'Haens, G.R. *et al.* Early lesions of recurrent Crohn's disease caused by infusion of intestinal contents in excluded ileum. *Gastroenterology* **114**, 262–267 (1998).
21. Cesaro, A. *et al.* Differential expression and regulation of ADAM17 and TIMP3 in acute inflamed intestinal epithelia. *Am. J. Physiol. Gastrointest. Liver Physiol.* **296**, G1332–G1343 (2009).
22. Cesaro, A. *et al.* Amplification loop of the inflammatory process is induced by P2X7R activation in intestinal epithelial cells in response to neutrophil transepithelial migration. *Am. J. Physiol. Gastrointest. Liver Physiol.* **299**, G32–G42 (2009).
23. Ogura, Y. *et al.* Expression of NOD2 in Paneth cells: a possible link to Crohn's ileitis. *Gut* **52**, 1591–1597 (2003).
24. Boudeau, J., Glasser, A.L., Masseret, E., Joly, B. & Darfeuille-Michaud, A. Invasive ability of an *Escherichia coli* strain isolated from the ileal mucosa of a patient with Crohn's disease. *Infect. Immun.* **67**, 4499–4509 (1999).

doi:10.1038/ng.762